

February 8, 2020  
ADP-01-31/T463  
JLAB-THY-01-22

## Parton Distributions from Lattice QCD

W. Detmold<sup>1</sup>, W. Melnitchouk<sup>1,2</sup> and A.W. Thomas<sup>1</sup>

<sup>1</sup> *Special Research Centre for the Subatomic Structure of Matter, and Department of Physics and Mathematical Physics, Adelaide University, 5005, Australia*

<sup>2</sup> *Jefferson Lab, 12000 Jefferson Avenue, Newport News, VA 23606*

### Abstract

We extract the  $x$  dependence of the valence nonsinglet  $u - d$  distribution function in the nucleon from the lowest few moments calculated on the lattice, using an extrapolation formula which ensures the correct behavior in the chiral and heavy quark limits. We discuss the implications for the quark mass dependence of meson masses lying on the  $J^{PC} = 1^{--}$  Regge trajectory.

## I. INTRODUCTION

Parton distribution functions (PDFs) contain a wealth of information on the nonperturbative structure of the nucleon. Quark and gluon distributions probed in deep inelastic scattering and other high energy processes have provided valuable insights into the workings of QCD in the low energy domain. The observation of an asymmetry between  $\bar{d}$  and  $\bar{u}$  quarks in the proton sea [1,2], to take just one example, has served to highlight the important role that the pion cloud of the nucleon and the chiral symmetry of QCD [3] plays in hadronic structure, even at high energies.

More generally, studies of PDFs can help with the task of identifying the appropriate effective degrees of freedom of QCD at low energies. Through the application of the operator product expansion (OPE) to QCD, high energy processes such as deep inelastic scattering can be factorized into short and long distance contributions, allowing one to calculate the former in perturbation theory, while isolating all of the nonperturbative physics in the latter. Over the past two decades considerable experience has been accumulated with various nonperturbative, low energy models of the nucleon which have been used to study PDFs [4]. Initial studies focused on the valence quark distributions as a means of constraining valence quark model parameters, although recently more ambitious efforts have attempted to describe sea quark and gluon distributions from low energy models.

Although the model studies have been helpful in exploring the relationship between high energy processes and low energy phenomenology, ultimately one would like a more exact connection of PDFs with QCD. A mathematically more rigorous approach is provided through lattice QCD. Indeed, the determination of the moments of the PDFs is one of the benchmark calculations of hadron structure in lattice QCD. Modern computational advances have allowed large scale simulations to be undertaken which are progressively improving the errors associated with finite lattice spacings and finite volume effects. However, until recently [5] large differences between lattice results and experiment have remained.

Because PDFs are light cone correlation functions, it is not possible to calculate them directly on the lattice in Euclidean space. Instead one calculates moments of PDFs, defined (for Björken  $x$ ) as:

$$\langle x^n \rangle_q = \int_0^1 dx x^n \left( q(x) + (-1)^{n+1} \bar{q}(x) \right) , \quad (1)$$

which are related through the OPE to matrix elements of local twist-two operators. A number of calculations of PDF moments have been performed over the last decade, most notably by the QCDSF group [6] in the quenched approximation. More recently, the MIT group [7] has confirmed the earlier quenched results, and in addition made the first unquenched simulations. These results indicate that at the relatively large quark masses at which the calculations were made, the unquenched results are indistinguishable from the quenched within the current errors.

Despite the impressive progress of lattice calculations of moments of PDFs, there has been a long standing problem in reconciling the lattice data with experiment, which has posed a serious threat to the credibility of current lattice calculations. Namely, for the unpolarized moments all of the calculations to date, which have been made at quark masses of between 30 and 190 MeV, have yielded results which are typically 50% larger than the

experimental values when linearly extrapolated to the physical quark masses. This discrepancy was recently resolved with the observation [5] that a linear extrapolation in quark mass omits crucial physics associated with the long range structure of the nucleon in the form of the pion cloud. In particular, the inclusion of the nonlinear, nonanalytic dependence on the quark mass in the extrapolation of the moments from the region of large quark masses to the physical, light quark masses allows one to fit both the lattice data and the experimental values with good accuracy [5]. It therefore restores confidence in the extraction of all hadron observables from current simulations.

In this paper we go one step further and ask what can the lattice data tell us about the  $x$  dependence of the PDFs themselves? In particular, we shall extract the valence nonsinglet distribution  $u_v - d_v$  by extrapolating the lattice data to the physical region using a form that ensures the correct behavior in the chiral and heavy quark limits. In Section II we examine the initial question of the extent to which the  $x$  dependence can be determined from just a few low moments of a PDF. After establishing the accuracy to which the PDF can be reconstructed, we then extract the valence  $u_v - d_v$  distribution from the calculated lattice moments in Section III. Using the chiral extrapolation formula, we compute the  $x$  dependence of the  $u_v - d_v$  distribution as a function of quark mass. In Section IV we discuss the implications of the results for masses of mesons lying on the  $J^{PC} = 1^{--}$  Regge trajectory. Finally, in Section V we make some concluding remarks.

## II. RECONSTRUCTION OF DISTRIBUTIONS FROM MOMENTS

The reconstruction of the complete  $x$  dependence of a PDF in principle requires infinitely many moments, so that *a priori* the task of building up a PDF from only a few, low moments may seem rather ambitious. This is especially true for PDFs at large  $x$ , information on which is contained in higher moments. On the lattice, because of problems with operator mixing for operators with spin  $\geq 5$ , all lattice calculations have so far been restricted to  $n \leq 3$ . It is crucial, therefore, if one is to ever make use of lattice data to learn about PDFs, to see which features of the PDFs can be reconstructed from just the lowest 3 or 4 moments.

Formally, the  $x$  dependence of the PDF can be obtained by performing an inverse Mellin transform of the moments. If enough moments are known (and can be continued to complex  $n$ ), one can make a reliable reconstruction of the distributions numerically (see e.g. Ref. [8]). However, since lattice data available at present (and in the foreseeable future) only exist for the first three nontrivial moments, this procedure becomes impractical. Alternatively, one can reconstruct the parameters in a given PDF parameterization by working with the moments directly. A similar method was applied to the reconstruction of polarized parton distributions in Ref. [9], while in Ref. [10] the  $x$  dependence of PDFs was investigated subject to constraints on their small- and large- $x$  behavior. In the present work, however, we wish to determine what constraints on the  $x$  dependence of the valence distribution are imposed by the actual lattice data.

A typical parameterization of quark (or antiquark) distributions used in global fits [11–13] is of the form:

$$xq(x) = ax^b(1-x)^c(1 + \epsilon\sqrt{x} + \gamma x) , \quad (2)$$

for which the corresponding moments are given by:

$$\langle x^n \rangle_q = a [B(1+c, b+n) + \epsilon B(1+c, \frac{1}{2}+b+n) + \gamma B(1+c, 1+b+n)] , \quad (3)$$

where  $B(x, y)$  is the  $\beta$ -function. For a given set of PDF moments, the parameters  $a, b, c, \epsilon$  and  $\gamma$  can be fitted using Eq. (3), and the corresponding  $x$  distribution obtained from Eq.(2). To test the effectiveness of this method, we calculate moments of PDFs from the recent MRS [11], CTEQ [12] and GRV [13] parameterizations, and examine how well the reconstructed distributions agree with the original parameterizations.

In order to make best use of currently available lattice data, we concentrate on the nonsinglet valence distribution  $u_v(x) - d_v(x) \equiv [u(x) - \bar{u}(x)] - [d(x) - \bar{d}(x)]$ . While the present analysis can be easily extended to the singlet sector, the singlet quark distribution on the lattice receives contributions from disconnected diagrams, corresponding to operator insertions in quark lines which are disconnected (except through gluon lines) from the nucleon source. Disconnected diagrams are considerably more difficult to compute, so only exploratory studies of these have so far been completed [14]. On the other hand, since the disconnected contributions are flavor independent (for equal  $u$  and  $d$  quark masses), they cancel exactly in the nonsinglet  $u - d$  combination.

To enable comparison with the reconstructed distributions, we employ Eq. (2) to construct an ‘average parameterization’ from the global PDF analyses. Note that the PDF fits in Refs. [11–13] are given for  $u_v(x)$  and  $d_v(x)$  separately, whereas here we require a parameterization of the difference. Using an equally weighted numerical fit to the  $u_v(x) - d_v(x)$  difference (at next-to-leading order in the  $\overline{\text{MS}}$  scheme, at a scale  $Q^2 = 4 \text{ GeV}^2$ ) from the parameterizations of Ref. [11–13], we find an average fit:

$$x(u_v(x) - d_v(x))_{\text{avg}} = a_\Delta x^{b_\Delta} (1 - x)^{c_\Delta} (1 + \epsilon_\Delta \sqrt{x} + \gamma_\Delta x) , \quad (4)$$

with  $b_\Delta = 0.476$ ,  $c_\Delta = 3.750$ ,  $\epsilon_\Delta = -3.152$ ,  $\gamma_\Delta = 16.64$ , and with  $a_\Delta = 0.561$  determined by the normalization condition,  $\int_0^1 dx (u_v(x) - d_v(x)) = 1$ . Figure 1 shows the average distribution (long-dashed line), with the spread between the three parameterizations indicated by the shaded region. The lowest six moments of this average valence  $u_v - d_v$  distribution are calculated to be:

$$\begin{aligned} \langle x^0 \rangle_{u_v-d_v}^{\text{avg}} &= 1 , & \langle x^1 \rangle_{u_v-d_v}^{\text{avg}} &= 0.163 , & \langle x^2 \rangle_{u_v-d_v}^{\text{avg}} &= 0.0543 , \\ \langle x^3 \rangle_{u_v-d_v}^{\text{avg}} &= 0.0229 , & \langle x^4 \rangle_{u_v-d_v}^{\text{avg}} &= 0.0111 , & \langle x^5 \rangle_{u_v-d_v}^{\text{avg}} &= 0.00599 . \end{aligned}$$

We have investigated fits to these moments using the following seven fitting functions: (i) the full form of Eq. (3) with unconstrained parameters; (ii) a simplified form with  $\gamma = 0$ ; (iii) a form with  $\epsilon = 0$ ; (iv) both  $\epsilon = 0$  and  $\gamma = 0$ ; (v) with the constraint  $\epsilon = \epsilon_\Delta$ ; (vi)  $\gamma = \gamma_\Delta$ ; and finally (vii)  $\epsilon = \epsilon_\Delta$  and  $\gamma = \gamma_\Delta$ . Fits (iii) and (iv) are unable to reproduce the small  $x$  behavior of the distribution and are therefore discarded. The parameters determined by  $\chi^2$  fits with each of the remaining forms give rise to similar distributions. We use the differences in the values of the parameters found from the various fits as an indication of the systematic error in the reconstruction procedure. In particular, for the parameter  $b$  (which is of special interest because of its relation to Regge phenomenology—see Section IV below), we find the best fit value  $b = 0.4 \pm 0.2$ .

Figure 1 shows the reconstructed  $x(u_v(x) - d_v(x))$  distribution (short-dashed line) which is generated by the fit form (i) using all six moments above. With just the lowest 4 moments,

however (as are available from lattice data), this form does not produce an accurate fit, as one is attempting to constrain more parameters than the number of data points permit<sup>1</sup>. This is illustrated by the dotted line in the Fig. 1. In contrast, with fit (vii), which has only 3 free parameters, one can obtain a fairly reliable reconstruction even when fitting to only the  $n = 0, 1, 2$  moments, as indicated by the solid curve in Figure 1.

As well as understanding the systematic uncertainty associated with the functional form of the distribution to be reconstructed, one must also quantify the error arising from the use of only a fixed number of moments. When the number of moments used with fitting form (vii) is increased to 4, 5 or 6 the fit improves by only a few percent. With four moments, fits (ii), (v) and (vi) also give acceptable results, similar to those shown for fit (vii). For simplicity, however, we will concentrate on fit form (vii) hereafter.

The overall agreement between the original and reconstructed distributions is clearly excellent, and comparable to the difference between different parameterizations (shaded region in Fig. 1). Having confidence that a reliable reconstruction is possible from just the lowest few moments, we next ask what do extrapolations of lattice data on the  $n = 0, 1, 2, 3$  moments tell us about the  $x$  dependence of the distribution  $u_v(x) - d_v(x)$ ?

### III. QUARK DISTRIBUTIONS FROM LATTICE MOMENTS

A crucial question for relating lattice calculations to phenomenology is the reliability of the extrapolation from the region of large quark masses ( $m_q$ ) to the physical value. Typically, lattice data have been analyzed assuming a linear dependence on the quark mass. However, as pointed out in Ref. [5], if one is to extrapolate the lattice moments into a region where pion loops play an important role, it is vital to use an extrapolation formula which has the correct chiral behavior. In this section we first motivate an extrapolation formula which ensures both the correct chiral and heavy quark limits. Following this, we use the values of the moments at physical quark masses extracted from the lattice data to reconstruct the  $x$  dependence of the nonsinglet distribution.

#### A. Constraints from the Chiral and Heavy Quark Limits

The spontaneous breaking of the chiral  $SU_L(N_f) \times SU_R(N_f)$  symmetry of QCD generates the nearly massless Goldstone bosons (pions), whose importance in hadron structure is well documented. At small pion masses, hadronic observables can be systematically expanded in a series in  $m_\pi$  [15]. The expansion coefficients are generally free parameters, determined from phenomenology or obtained from low energy models. One of the unique consequences of pion loops, however, is the appearance of so-called chiral logs. From the Gell-Mann–Oakes–Renner relation one finds that  $m_\pi^2 \sim m_q$  at small  $m_\pi$ , so that these terms are nonanalytic functions of the quark mass. Because the nonanalytic terms arise from the infra-red behavior of the

---

<sup>1</sup>Here we count the zeroth moment as a fit point with zero error, and include the overall normalization parameter  $a$  in our parameter counting.

chiral loops, they are generally model independent. For some observables these nonanalytic terms give rise to large deviations from linearity near the chiral limit [16].

The leading order (in  $m_\pi$ ) nonanalytic term in the expansion of the moments of PDFs was shown in Ref. [3] to have the generic behavior  $m_\pi^2 \log m_\pi$ . In Ref. [5] a low order chiral expansion for the moments of the nonsinglet  $u - d$  distribution was developed which incorporated the leading nonanalytic (LNA) behavior of the moments as a function of  $m_q$ . Here we extend this in order to connect also with the heavy quark limit, in which the valence quark distributions become  $\delta$ -functions centered at  $x = 1/3$ :

$$u(x) - d(x) \xrightarrow{m_q \rightarrow \infty} \delta(x - \frac{1}{3}) . \quad (5)$$

The corresponding moments in the heavy limit are therefore given by:

$$\langle x^n \rangle_{u-d} \xrightarrow{m_q \rightarrow \infty} \frac{1}{3^n} . \quad (6)$$

It is straightforward to incorporate this constraint into the extrapolation formula, and its inclusion makes no significant difference to the central results of Ref. [5], as illustrated in Fig. 2. For completeness, we give the extrapolation formula which explicitly satisfies both the heavy quark and chiral limits:

$$\langle x^n \rangle_{u-d} = a_n \left( 1 + c_{\text{LNA}} m_\pi^2 \log \frac{m_\pi^2}{m_\pi^2 + \mu^2} \right) + b_n \frac{m_\pi^2}{m_\pi^2 + m_{b,n}^2} , \quad (7)$$

where the coefficient  $c_{\text{LNA}} = -(1 + 3g_A^2)/(4\pi f_\pi)^2$  [17], and  $b_n$  is a constant constrained by Eq.(6):

$$b_n = \frac{1}{3^n} - a_n \left( 1 - \mu^2 c_{\text{LNA}} \right) . \quad (8)$$

In this extrapolation scheme there are therefore three free parameters for each moment:  $a_n$ ,  $m_{b,n}$ , and  $\mu$ . We find that the dependence of the mass parameter  $m_{b,n}$  on  $n$  is quite small, and therefore fix  $m_{b,n} = m_b$  for all  $n$ . As the  $b_n$  term in Eq. (7) is included in order to provide a linear dependence on  $m_\pi^2$  in the region where lattice data exist,  $m_b$  should be large enough such that this is indeed the case. For  $m_b > 4$  GeV the fits to the moments are essentially independent of  $m_b$ ; we therefore fix  $m_b = 5$  GeV.

The mass  $\mu$  essentially determines the scale above which pion loops no longer yield rapid variation. Analyses of a wide range of observables such as masses, magnetic moments and charge radii [16] as well as structure function moments suggest a common scale,  $\mu \sim 0.5$  GeV, which simply reflects the scale at which the Compton wavelength of the pion becomes comparable to the size of the hadron (without its pion cloud). We use the value  $\mu = 550$  MeV found in our previous fits to the lattice moments of the  $u - d$  distributions in Ref. [5]. Consequently the extrapolation for each moment is essentially parameterized by only one variable. Nevertheless, the best fit using Eq.(6) is as good as that found in our earlier work [5] (which did not impose the additional constraint of the heavy quark limit), as illustrated in Fig. 2 — the latter is given by the short-dashed curve and the former by the solid curve. For details of the fitting procedure and the error analysis we refer to Ref. [5].

Having motivated the functional form of the extrapolation formula to connect with both the chiral and heavy quark limits, we now use the extracted moments to calculate the  $x$  dependence of the nonsinglet valence  $u - d$  distribution from the lattice data.

## B. Results

Before extracting information on the  $x$  dependence of a particular PDF from the lattice moments, one must note that the crossing symmetry properties of the spin-averaged quark distributions (see Eq. (1)) mean that the moments of  $u - d$  calculated on the lattice correspond to the *valence*  $u_v - d_v$  distribution only for *even*  $n$ . The *odd*  $n$  moments, on the other hand, correspond to the combination  $u + \bar{u} - d - \bar{d} = u_v - d_v - 2(\bar{d} - \bar{u})$ . The difference between the two represents the famous violation of the Gottfried sum rule, when  $\bar{d} \neq \bar{u}$  [1,2]. Some care must be taken, therefore, if one attempts to use information on both even and odd moments to extract a valence quark distribution. To minimize possible contamination of the extracted valence distribution arising from the flavor asymmetry of the sea, in the present analysis we subtract the values of the phenomenological moments of the  $\bar{d} - \bar{u}$  difference, as given by global parameterizations of data [11–13], from the calculated odd moments.

Phenomenologically, the difference  $\bar{d}(x) - \bar{u}(x)$  is found to be concentrated at small  $x$  ( $\bar{d} - \bar{u} \sim (1-x)^{14}$  at  $Q^2 \sim 50$  GeV $^2$  from the Fermilab Drell-Yan data [2]), and will therefore become progressively less important for larger  $n$  compared with the valence distribution. The largest effect is for the  $n = 1$  moment and results in a correction of  $< 10\%$  of the value of  $\langle x \rangle_{u-d}$  in Eq. (5), if one adds the phenomenological value  $2 \int_0^1 x(\bar{d}(x) - \bar{u}(x))dx = 0.017(2)$  [11–13] to the extrapolated first moment. For the  $n = 3$  moment, the corresponding correction is a fraction of a percent. In principle, given sufficiently many moments, one can fit *both* the total  $u - d$  and valence  $u_v - d_v$  distributions separately from the  $n$  even and  $n$  odd moments, respectively — however, given the small number of moments currently available, the extraction of the valence distribution is the most feasible solution.

Table I lists the resulting extrapolated values for the lowest three nontrivial moments of the *total*  $u - d$  distribution at the physical quark mass for both a linear extrapolation and the chirally symmetric extrapolation of Eq. (7). Also listed are the corresponding values of the valence fit parameters  $a$ ,  $b$  and  $c$  from  $\chi^2$  fits. As discussed in Section II, because there are only four data points with which to fix parameters, we use Eq. (3) with the fitting form (vii), namely fixing  $\epsilon = \epsilon_\Delta$  and  $\gamma = \gamma_\Delta$ . With these parameters, the resulting fits to the moments of the *valence*  $u_v - d_v$  distribution are displayed in Fig. 3 for both the linear and improved, chirally symmetric extrapolation. For clarity we plot  $3^n$  times the moments, so that the horizontal line at unity represents the heavy quark limit of the moments. The lightly shaded region around the moments from the improved chiral extrapolation corresponds to a 1 standard deviation variation of the fit parameters from their optimal values.

The corresponding distributions  $x(u_v(x) - d_v(x))$  are displayed in Fig. 4. Once again, the lightly shaded region represents a  $1\sigma$  deviation from the central values, while the darker band illustrates the spread between the global parameterizations from Refs. [11–13]. A comparison of the distribution reconstructed from the lattice data using the improved chiral extrapolation with the phenomenological distributions shows reasonably good agreement. On the other hand, the linear extrapolation gives a distribution (scaled by a factor 1/2 in the figure) which is much smaller than the phenomenological distributions at small  $x$ , and consequently has a significantly higher peak in the intermediate  $x$  region, centered at  $x \sim 1/3$  — reminiscent of a heavy, constituent quark-like distribution.

The improved extrapolation formula (7) enables one to study not only the quark distribution at the physical quark mass, but also the dependence of the distribution on the quark

(or equivalently, pion) mass. In particular, it allows one to trace how the  $x$  dependence changes as one goes from the chiral limit to the heavy quark limit, where the distribution approaches a  $\delta$ -function. Table II lists the extrapolated values of the total moments at various pion masses. Fitting the corresponding valence moments with the functional form (vii) from Section II, this table also shows how the resulting fit parameters change as the pion mass is increased from  $m_\pi = 0$  to  $m_\pi = 5$  GeV. Notice that the fit parameters  $b$  and  $c$  become larger with increasing  $m_\pi$ , as the  $x$  dependence of the valence distribution becomes less singular at small  $x$ . This is dramatically illustrated in Fig. 5, where the corresponding valence  $x(u_v - d_v)$  distribution is shown in the chiral limit ( $m_\pi = 0$ ), at the physical mass ( $m_\pi = 0.139$  GeV), and at  $m_\pi = 0.5, 1$  and  $5$  GeV. As  $m_\pi$  increases, the distribution becomes visibly more sharply peaked, with the peak moving towards the limiting value of  $x = 1/3$ .

Quite remarkably, the distribution at  $m_\pi = 5$  GeV resembles the distribution in Fig. 4 (dot-dashed curve) extracted from the linearly extrapolated moments. Since the linearly extrapolated moments are not constrained by the expected behavior in the heavy quark limit, it is noteworthy that a constituent quark-like distribution, peaking near  $x \sim 1/3$ , nevertheless arises if the moments are flat as a function of  $m_\pi$ , as one would expect within a constituent quark model. This in fact provides further *a posteriori* justification for the choice made in Eq.(7) to build in the correct heavy quark limit (as well as the correct chiral behavior).

#### IV. REGGE BEHAVIOR AND THE $J^{PC} = 1^{--}$ TRAJECTORY

In the previous section we extracted the exponent  $b$  which governs the small- $x$  behavior of the nonsinglet valence quark distribution  $u_v - d_v$ . According to Regge theory [18], this exponent is related to the slope of the isovector  $J^{PC} = 1^{--}$  trajectory, corresponding to the exchange of  $\rho$  ( $1^{--}$ ),  $a_2$  ( $2^{++}$ ),  $\rho_3$  ( $3^{--}$ ) and so on. If one makes the reasonable hypothesis that Regge theory also holds for quarks with masses in the range  $m_q \sim 30$ –190 MeV used in lattice simulations, one can estimate the masses of mesons on this trajectory from fits to the valence quark moments versus  $m_q$ .

From Regge theory the elastic scattering amplitude at high center of mass energy,  $s$ , behaves as:

$$\mathcal{A}(s, t) \sim s^{\alpha(t)}, \quad (9)$$

where  $\alpha(t)$  is a function describing the meson trajectory:

$$\alpha(t) = \alpha_0 + \alpha' t, \quad (10)$$

with  $\alpha'$  the slope and  $\alpha_0$  the intercept of the trajectory. The optical theorem then relates the imaginary part of the scattering amplitude at forward angles,  $\mathcal{A}(s, t = 0)$ , to the total cross section,  $\sigma$ :

$$\sigma \sim \frac{\text{Im} \mathcal{A}}{s} \sim s^{\alpha_0 - 1}. \quad (11)$$

At large  $s$  the approximate energy independence of total cross sections is usually attributed to the exchange of the Pomeron (IP) trajectory, which has intercept  $\alpha_0^{\text{IP}} \approx 1$ . On the other

hand, the isovector cross sections (corresponding to nonsinglet distributions) are dominated by the exchange of a trajectory with  $\bar{q}q$  quantum numbers corresponding to the  $\rho$  meson and its excitations, which has intercept  $\alpha_0^\rho \approx 0.5$ .

In deep-inelastic scattering at large  $s \gg Q^2$ , corresponding to  $x = Q^2/2p \cdot q \sim Q^2/s \ll 1$ , the total virtual photon–nucleon cross section is dominated by the singlet quark and gluon distributions, and behaves as  $\sigma^{\gamma^* N} \sim F_2^N \sim x^{1-\alpha_0^P}$ . The nonsinglet distribution,  $q_{NS}$ , on the other hand, is governed by the exchange of the  $J^{PC} = 1^{--}$  trajectory,  $xq_{NS} \sim x^{1-\alpha_0^\rho} \sim x^{1/2}$  (recall that the best fit to the average  $u_v - d_v$  difference in Eq. (4) gave an exponent  $b = 0.476$ ). Identifying  $\alpha_0^\rho \approx 1 - b$  from the previous section as a function of quark mass, one can therefore extract information on the  $m_q$  dependence of the Regge intercept from the  $m_q$  dependence of the nonsinglet quark distribution.

Having determined the intercept  $b \approx 1 - \alpha_0^\rho$  from the PDF fits, one needs to determine the slope of the trajectory as a function of  $m_q$ . In the infinite mass limit, orbital excitations of mesons become energetically degenerate with the  $L = 0$  state. Within the Regge picture, this is possible only if the Regge intercept  $\alpha_0^\rho \xrightarrow{m_q \rightarrow \infty} -\infty$ , or  $b \xrightarrow{m_q \rightarrow \infty} \infty$ , which is consistent with the valence distribution approaching a  $\delta$ -function. One expects, therefore, that the slope  $\alpha'$  should increase as  $m_q$  increases from its physical value. The behavior  $\alpha_0^\rho \xrightarrow{m_q \rightarrow \infty} -\infty$  is indeed what is seen from the  $m_\pi$  dependence of  $b$  in Table II. The slope at larger, but finite, values of  $m_q$  is most accurately determined from the mass of the  $\rho$  meson, which has considerably smaller errors than the masses of higher lying mesons on the same trajectory. Using the lattice data for the  $\rho$  meson and the values of  $\alpha_0^\rho(m_q)$  generated from the fits in Section III, one can then make predictions for the behavior of the masses of the orbital excitations as a function of  $m_q$ .

In Fig. 6 we show the predicted  $1^{--}$  Regge trajectory at  $m_\pi = 0.785$  GeV (solid line), compared with the trajectory at the physical light quark mass (dashed). A fit through the central values of the parameter  $b$  and the  $\rho$  mass at  $m_\pi = 0.785$  GeV (as calculated in Ref. [19]) yields a slope which is somewhat larger than that of the trajectory at the physical quark mass, which is consistent with the expected trend towards the heavy quark limit. The darker shaded region represents the statistical error in the extrapolation of the lattice moments, obtained from fitting the upper and lower bounds of the original lattice data. The lighter region indicates an estimate of the systematic error associated with the fitting procedure as discussed in Section II.

Although lattice data for the masses of orbital excitations are scarce, there have been some pioneering calculations of masses of the  $a_2$  ( $J^{PC} = 2^{++}$ ) and  $\rho_3$  ( $J^{PC} = 3^{--}$ ) mesons by the UKQCD Collaboration [19], indicated by the filled boxes in Fig. 6. Comparing with the predictions from the PDF analysis, the lattice data are in reasonable agreement: the calculated  $\rho_3$  meson mass lies within the predicted band, albeit within large errors, while the  $a_2$  mass lies on the edge of the predicted range. Needless to say, further exploration of the masses of excited mesons within lattice QCD would be very helpful in testing these predictions.

## V. CONCLUSION

In this paper we have extracted the  $x$  dependence of the unpolarized valence quark distribution  $x(u_v(x) - d_v(x))$  from lattice QCD data on the moments of the  $u - d$  distribution.

After establishing that the basic features of the  $x$  distributions can be reconstructed from just the lowest four moments, we analyze the lattice data using an extrapolation formula which embodies the correct behavior in both the chiral and heavy quark limits.

The importance of ensuring the correct chiral behavior is illustrated by comparing the  $x$  distributions obtained by extrapolating the lattice data using a linear and an improved chiral extrapolation. While the improved extrapolation gives an  $x$  distribution which is in quite good agreement with the phenomenological parameterizations, the linearly extrapolated data give rise to distributions with the wrong small- $x$  behavior, which translates into a much more pronounced peak at  $x \sim 1/3$ , reminiscent of a heavy, constituent quark-like distribution. The approach to the heavy quark limit is explicitly mapped out by studying the dependence of the  $x$  distributions on the pion mass, from the chiral limit to pion masses of several GeV.

Our analysis suggests an intriguing connection between the small- $x$  behavior of the valence distributions and the  $m_q$  dependence of meson masses on the  $J^{PC} = 1^{--}$  trajectory. While the existing lattice data are in qualitative agreement with the predictions from the PDF analysis, future results on the masses of excited meson states at varying quark mass will enable the accuracy of this relation to be tested more thoroughly. Plans by a number of lattice groups to study the spectrum of excited hadrons should provide valuable insights into this problem.

## ACKNOWLEDGMENTS

We would like to thank D.B. Leinweber and C. Michael for helpful discussions and communications. This work was supported by the Australian Research Council, and the U.S. Department of Energy contract DE-AC05-84ER40150, under which the Southeastern Universities Research Association (SURA) operates the Thomas Jefferson National Accelerator Facility (Jefferson Lab).

## REFERENCES

- [1] P. Amaudruz *et al.*, Phys. Rev. Lett. **66**, 2712 (1991).
- [2] E.A. Hawker *et al.*, Phys. Rev. Lett. **80**, 3715 (1998); J.C. Peng *et al.*, Phys. Rev. D **58**, 092004 (1998).
- [3] A.W. Thomas, W. Melnitchouk and F.M. Steffens, Phys. Rev. Lett. **85**, 2892 (2000); A.W. Thomas, Phys. Lett. B **126**, 97 (1983).
- [4] A.W. Thomas and W. Weise, *The Structure of the Nucleon* (Wiley-VCH, Berlin 2001).
- [5] W. Detmold, W. Melnitchouk, J. W. Negele, D. B. Renner and A. W. Thomas, hep-lat/0103006.
- [6] M. Göckeler *et al.*, Phys. Rev. D **53**, 2317 (1996); M. Göckeler *et al.*, Nucl. Phys. Proc. Suppl. **53**, 81 (1997); C. Best *et al.*, hep-ph/9706502.
- [7] D. Dolgov *et al.*, hep-lat/0011010, and to be published.
- [8] T. Weigl and W. Melnitchouk, Nucl. Phys. B **465**, 267 (1996).
- [9] M. Göckeler *et al.*, hep-ph/9711245.
- [10] T. Weigl and L. Mankiewicz, Phys. Lett. B **389**, 334 (1996).
- [11] A.D. Martin, R.G. Roberts, W.J. Stirling and R.S. Thorne, Eur. Phys. J. C **14**, 133 (2000).
- [12] H.L. Lai *et al.*, Eur. Phys. J. C **12**, 375 (2000).
- [13] M. Glück, E. Reya and A. Vogt, Eur. Phys. J. C **5**, 461 (1998).
- [14] S.J. Dong, K.F. Liu and A.G. Williams, Phys. Rev. D **58**, 074504 (1998); S. Güsken *et al.*, hep-lat/9901009. W. Wilcox, Nucl. Phys. Proc. Suppl. **94**, 319 (2001).
- [15] S. Weinberg, Physica (Amsterdam) **96 A**, 327 (1979); J. Gasser and H. Leutwyler, Ann. Phys. **158**, 142 (1984).
- [16] D.B. Leinweber and T.D. Cohen, Phys. Rev. D **47**, 2147 (1993); E.J. Hackett-Jones, D.B. Leinweber and A.W. Thomas, Phys. Lett. B **494**, 89 (2000); D.B. Leinweber, D.H. Lu and A.W. Thomas, Phys. Rev. D **60**, 034014 (1999); D.B. Leinweber and A.W. Thomas, *ibid.* D **62**, 074505 (2000).
- [17] D. Arndt and M.J. Savage, nucl-th/0105045; J.-W. Chen and X. Ji, hep-ph/0105197.
- [18] P.D.B. Collins, *An Introduction to Regge Theory and High Energy Physics* (Cambridge University Press, 1977).
- [19] P. Lacock, C. Michael, P. Boyle and P. Rowland, Phys. Rev. D **54**, 6997 (1996).

## TABLES

Extrapolation	$\langle x^1 \rangle$	$\langle x^2 \rangle$	$\langle x^3 \rangle$	$a$	$b$	$c$
Linear	0.262	0.0843	0.0340	658	3.51	10.5
Improved	0.149	0.0461	0.0200	0.439	0.351	3.77

TABLE I. Moments of the *total*  $u - d$  distribution obtained from a linear extrapolation and the improved chirally symmetric extrapolation, Eq. (7), to the physical quark mass. Also shown are the best fit parameters  $a$ ,  $b$  and  $c$  for the *valence*  $u_v(x) - d_v(x)$  distribution, using Eq. (3) with  $\epsilon = \epsilon_\Delta$  and  $\gamma = \gamma_\Delta$  constrained to the average values (see text).

$m_\pi$ (GeV)	$\langle x^1 \rangle$	$\langle x^2 \rangle$	$\langle x^3 \rangle$	$a$	$b$	$c$
0	0.121	0.0374	0.0161	0.282	0.245	3.55
$m_\pi^{\text{phys}}$	0.149	0.0461	0.0200	0.439	0.351	3.77
0.5	0.223	0.0689	0.0296	2.39	0.957	4.96
0.785	0.248	0.0769	0.0328	7.30	1.45	5.91
1	0.258	0.0801	0.0341	13.8	1.74	6.48
5	0.303	0.0978	0.0367	125000	6.20	15.4

TABLE II. Moments of the *total*  $u - d$  distribution obtained from the improved chiral extrapolation formula, Eq. (7), at various pion masses; and best fit parameters for the corresponding *valence*  $u_v(x) - d_v(x)$  distribution using Eq. (3) with  $\epsilon = \epsilon_\Delta$  and  $\gamma = \gamma_\Delta$  constrained to the average values.

## FIGURES

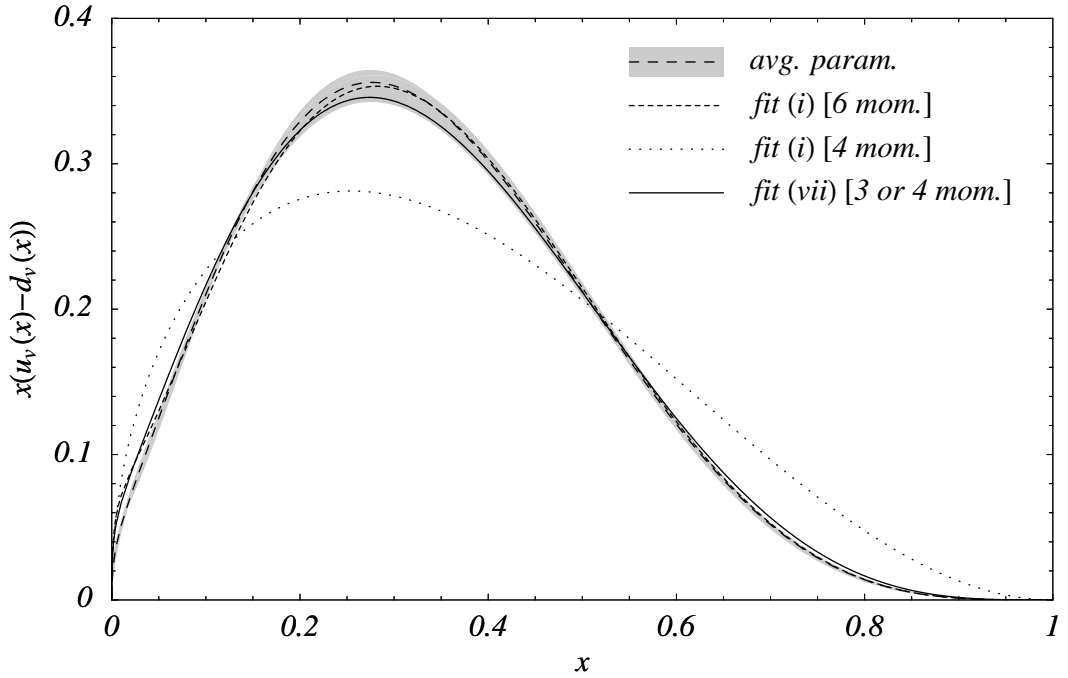


FIG. 1. Quality of reconstruction of the valence  $x(u_v(x) - d_v(x))$  distribution from several low moments: the shaded region represents the spread between different next-to-leading order distributions from global parameterizations [11–13] (at  $Q^2 = 4$  GeV $^2$  in the  $\overline{\text{MS}}$  scheme), while the long-dashed line represents a parameterization of the average of the three distributions, Eq. (4). The short-dashed line (which is almost indistinguishable from the long-dashed, average parameterization) is the distribution reconstructed from the lowest six moments of the average parameterization using Eq. (3) with  $\epsilon$  and  $\gamma$  unconstrained. The dotted curve indicates the fit obtained when only four moments are used with the same fitting form. In contrast, the solid lines represent the distribution reconstructed from the lowest three moments ( $n = 0, 1, 2$ ) using Eq. (3) with  $\epsilon$  and  $\gamma$  constrained to the values obtained from direct fits to the average distribution,  $\epsilon = \epsilon_\Delta$  and  $\gamma = \gamma_\Delta$ .

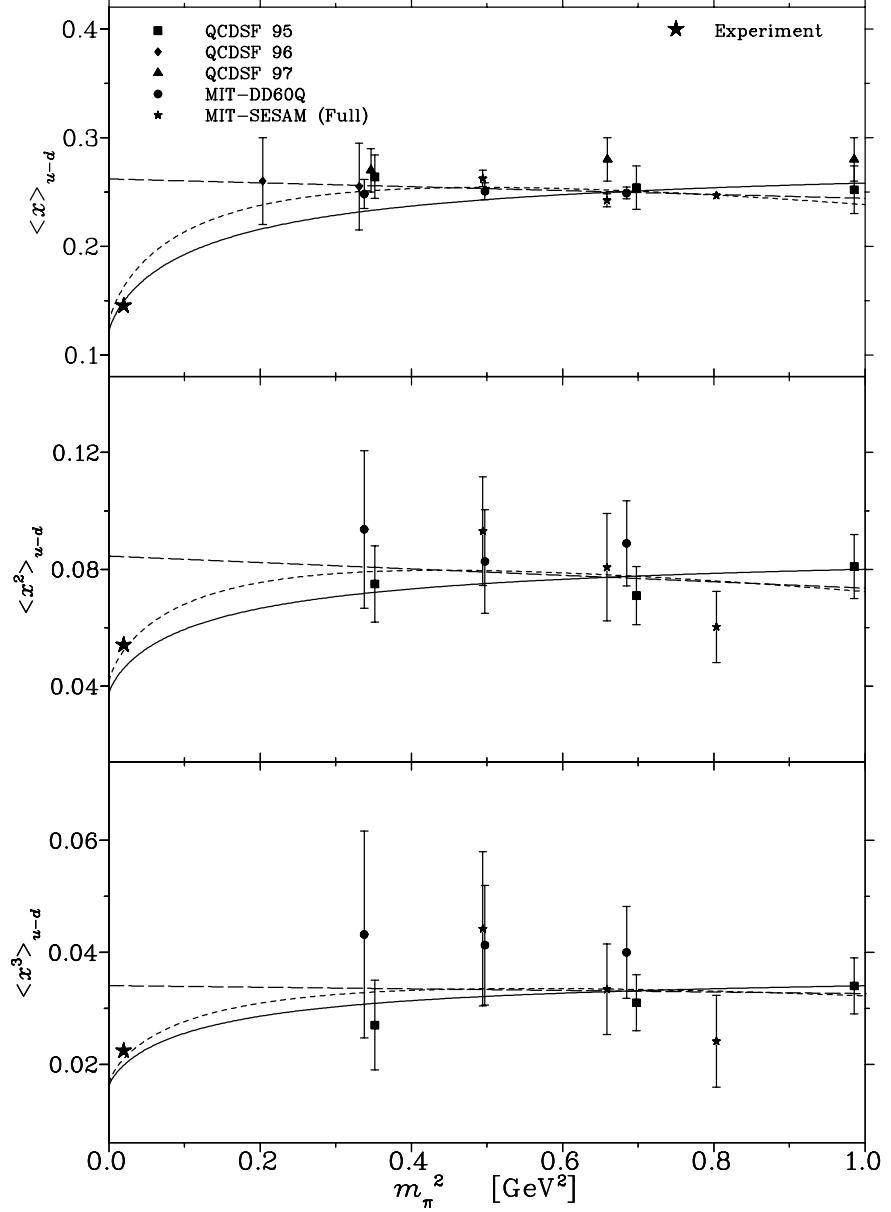


FIG. 2. Moments of the  $u - d$  distribution. The lattice data [6,7] are fitted using a linear function (long-dashed), and with the improved chiral extrapolation in Eq. (7) (solid). Also shown is the fit from Ref. [5] (short-dashed) which does not impose the heavy quark limit, Eq.(6).

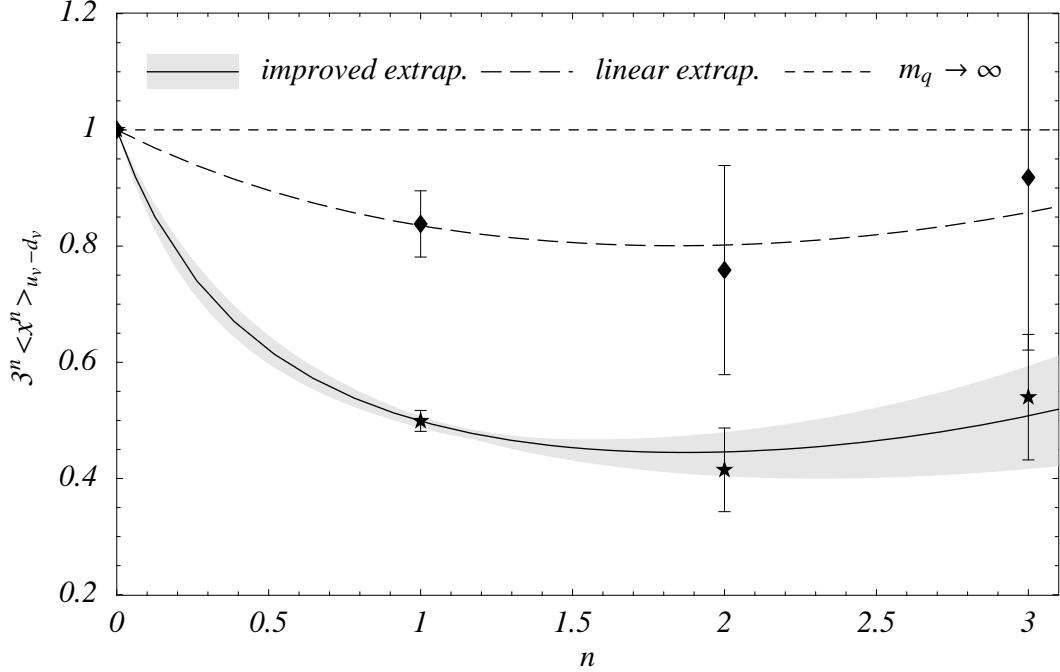


FIG. 3. The lowest four moments of the valence  $u_v - d_v$  distribution (scaled by  $3^n$ ) at the physical quark mass, extracted from the fit to the lattice data using a linear extrapolation (diamonds) and the improved chiral extrapolation, Eq. (7) (stars). The solid and dot-dashed lines are  $\chi^2$  fits to the improved and linearly extrapolated moments respectively using Eq. (3), with  $\epsilon$  and  $\gamma$  constrained to their average values. The shaded region represents a 1 standard deviation of the fit parameters about the optimal values for the improved extrapolation. The short-dashed line represents the heavy quark limits of the moments.

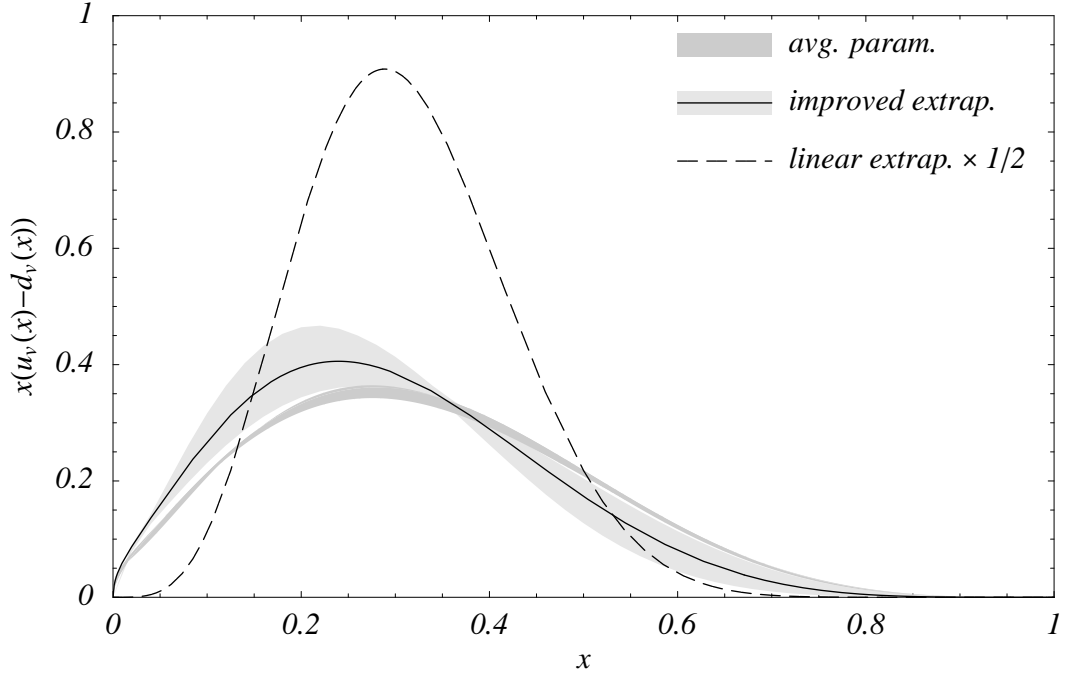


FIG. 4. The physical valence  $x(u_v(x) - d_v(x))$  distribution, extracted using the improved chiral extrapolation of the lattice moments (solid), and a linear extrapolation, scaled by a factor 1/2 (dot-dashed). The lighter shaded region indicates a  $1\sigma$  variation of the fit parameters about the optimal values for the improved extrapolation, while the dark shaded region represents the spread between global parameterizations [11–13].

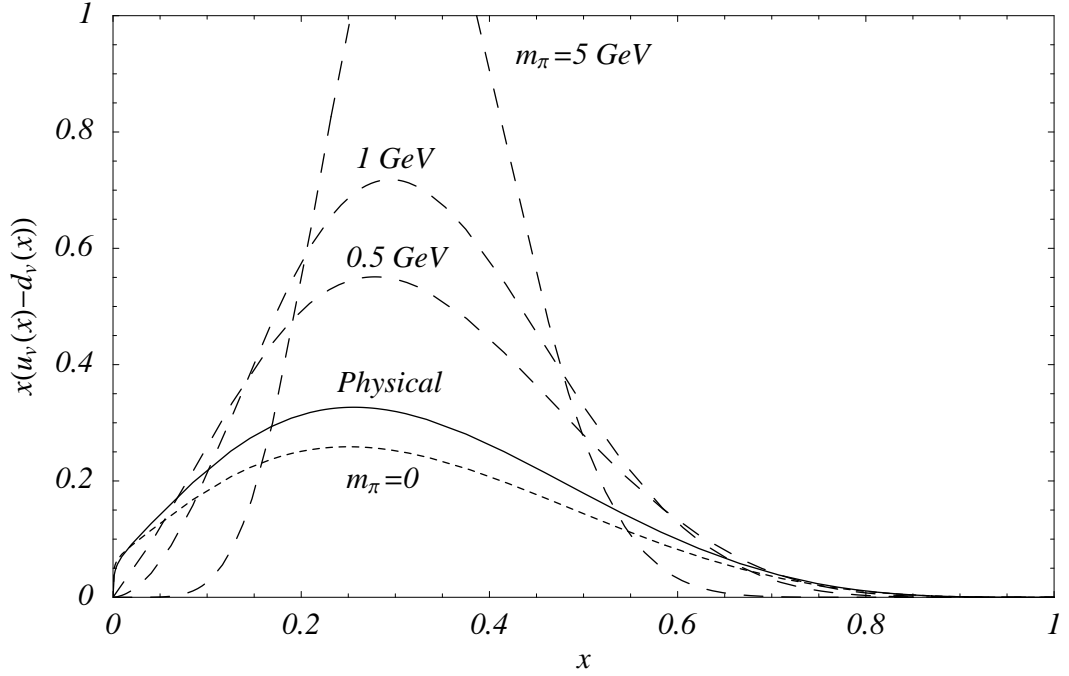


FIG. 5. The nonsinglet valence distribution  $x(u_v(x) - d_v(x))$  extracted from the improved extrapolation formula, Eq. (7), for various pion masses:  $m_\pi = 0$  (short-dashed),  $m_\pi = 0.139$  GeV (solid),  $m_\pi = 0.5$ , 1 and 5 GeV (long-dashed). The fit parameters are tabulated in Table II.

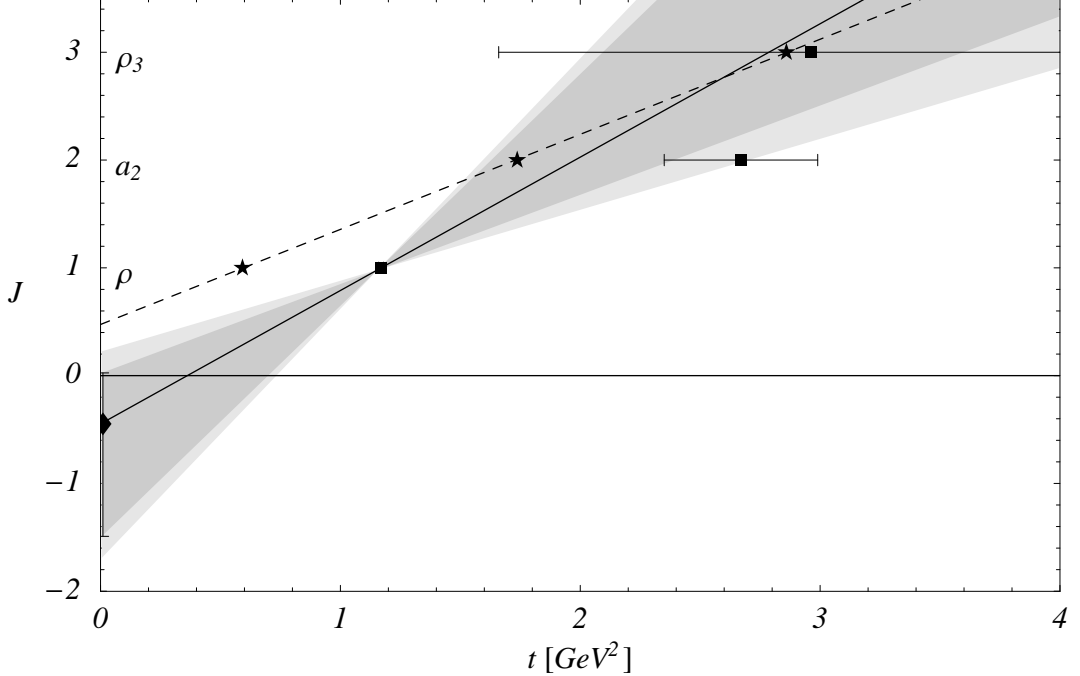


FIG. 6. Regge plot of the spin,  $J = \alpha_0^\rho$ , versus  $t = (\text{mass})^2$  of mesons on the  $J^{PC} = 1^{--}$  trajectory, at the physical pion mass (dashed) and at  $m_\pi = 785$  MeV (solid), with the point at  $t = 0$  obtained from the best fit to  $b$  (see Table II). The darker shaded region, which includes the error on  $b$ , illustrates the statistical error in the extrapolation of the lattice moments, while the lighter shaded region indicates the systematic error in the fitting procedure. The physical masses of the  $\rho$ ,  $a_2$  and  $\rho_3$  mesons are indicated by stars, while the boxes represent lattice masses at  $m_\pi = 0.785$  GeV from the UKQCD Collaboration [19].